JCI The Journal of Clinical Investigation

NADPH oxidase 4 limits bone mass by promoting osteoclastogenesis

Claudia Goettsch, … , Ralf P. Brandes, Katrin Schröder

J Clin Invest. 2013;123(11):4731-4738. https://doi.org/10.1172/JCI67603.

Research Article **Bone biology**

ROS are implicated in bone diseases. NADPH oxidase 4 (NOX4), a constitutively active enzymatic source of ROS, may contribute to the development of such disorders. Therefore, we studied the role of NOX4 in bone homeostasis. *Nox4*$^{-/-}$ mice displayed higher bone density and reduced numbers and markers of osteoclasts. Ex vivo, differentiation of monocytes into osteoclasts with RANKL and M-CSF induced *Nox4* expression. Loss of NOX4 activity attenuated osteoclastogenesis, which was accompanied by impaired activation of RANKL-induced NFATc1 and c-JUN. In an in vivo model of murine ovariectomy–induced osteoporosis, pharmacological inhibition or acute genetic knockdown of *Nox4* mitigated loss of trabecular bone. Human bone obtained from patients with increased osteoclast activity exhibited increased NOX4 expression. Moreover, a SNP of *NOX4* was associated with elevated circulating markers of bone turnover and reduced bone density in women. Thus, NOX4 is involved in bone loss and represents a potential therapeutic target for the treatment of osteoporosis.

NADPH oxidase 4 limits bone mass by promoting osteoclastogenesis

Claudia Goettsch,[1,2] Andrea Babelova,[3] Olivia Trummer,[4] Reinhold G. Erben,[5] Martina Rauner,[1] Stefan Rammelt,[6,7] Norbert Weissmann,[8] Valeska Weinberger,[3] Sebastian Benkhoff,[3] Marian Kampschulte,[9] Barbara Obermayer-Pietsch,[4] Lorenz C. Hofbauer,[1,7] Ralf P. Brandes,[3] and Katrin Schröder[3]

[1]Division of Endocrinology, Diabetes, and Bone Diseases, Department of Medicine III, Technical University, Dresden, Germany. [2]Center for Interdisciplinary Cardiovascular Sciences, Department of Medicine, Brigham and Women's Hospital, Harvard Medical School, Boston, Massachusetts, USA. [3]Institute of Physiology I, Goethe-University, Frankfurt, Germany. [4]Division of Endocrinology and Metabolism, Department of Internal Medicine, Medical University of Graz, Graz, Austria. [5]University of Veterinary Medicine, Vienna, Austria. [6]Department of Trauma and Reconstructive Surgery, Technical University, Dresden, Germany. [7]Center for Regenerative Therapies Dresden, Dresden, Germany. [8]University of Giessen Lung Center, Giessen, Germany. [9]Universitätsklinikum Gießen und Marburg GmbH — Standort Gießen, Zentrum für Radiologie, Abteilung für Radiologie, Marburg, Germany.

ROS are implicated in bone diseases. NADPH oxidase 4 (NOX4), a constitutively active enzymatic source of ROS, may contribute to the development of such disorders. Therefore, we studied the role of NOX4 in bone homeostasis. *Nox4*$^{-/-}$ mice displayed higher bone density and reduced numbers and markers of osteoclasts. Ex vivo, differentiation of monocytes into osteoclasts with RANKL and M-CSF induced *Nox4* expression. Loss of NOX4 activity attenuated osteoclastogenesis, which was accompanied by impaired activation of RANKL-induced NFATc1 and c-JUN. In an in vivo model of murine ovariectomy–induced osteoporosis, pharmacological inhibition or acute genetic knockdown of *Nox4* mitigated loss of trabecular bone. Human bone obtained from patients with increased osteoclast activity exhibited increased NOX4 expression. Moreover, a SNP of *NOX4* was associated with elevated circulating markers of bone turnover and reduced bone density in women. Thus, NOX4 is involved in bone loss and represents a potential therapeutic target for the treatment of osteoporosis.

Introduction

Bone is a dynamic organ that undergoes constant remodeling in response to external stimuli. While bone formation is mediated by osteoblasts, bone resorption is performed by osteoclasts, which derive from the myeloid lineage. In vivo as well as in cell culture models, osteoclastogenesis requires the differentiation factors RANKL and M-CSF (1). M-CSF induces the expression of RANK, the receptor of RANKL on myeloid cells. RANKL binding initiates osteoclast differentiation and activation (2) and is responsible for the induction of osteoclastic genes like tartrate-resistant acid phosphatase (TRAP) and cathepsin K (3). Mature osteoclasts are also activated by RANKL, which maintains their survival (4) and induces cytoskeletal rearrangement, promoting bone resorption (5).

Osteoclastogenesis can also be promoted by cytokines like TGF-β, which act in a biphasic manner on osteoclast formation (6). TGF-β has been linked to oxidative stress, as it increases the formation of ROS and induces the expression of NADPH oxidase 4 (NOX4) (7).

In the NOX family, whose sole function is to produce ROS, NOX4 takes an exceptional position. NOX4 is induced in the course of differentiation in many cells and is constitutively active. Thus, ROS production by NOX4 is largely controlled by the expression level of the enzyme. NOX4 produces H_2O_2 (8), whereas other NOX proteins generate superoxide anions, require complex activation steps, and show tissue-specific expression. The permanent production of H_2O_2 by NOX4 potentially adjusts the cellular redox status and interferes with slow processes like differentiation of mesenchymal cells, such as cardiac myocytes, smooth muscle cells, or adipocytes (9).

It has long been suggested that ROS stimulate osteoclasts (10), and impaired antioxidative defense is thought to contribute to increased bone resorption (11). Increased ROS production has also been linked to osteoclastogenesis in cell culture models (12, 13), but the enzymatic source and mechanisms of ROS-induced osteoclastogenesis have not been deciphered.

In the present study, we showed that NOX4 contributes to osteoclastogenesis, that loss of NOX4 activity prevents bone loss in mice, and that NOX4 is associated with increased parameters of bone resorption in humans.

Results

NOX4 negatively affects bone density in mice by increasing osteoclast numbers. To identify the effect of NOX4 on bone homeostasis, WT and *Nox4*$^{-/-}$ mice were studied. As confirmed by Western blot analysis, NOX4 expression was apparent in femur lysates of WT mice, but not *Nox4*$^{-/-}$ mice (Supplemental Figure 1; supplemental material available online with this article; doi:10.1172/JCI67603DS1). Bones of *Nox4*$^{-/-}$ mice displayed greater trabecular width and thickness than those of WT mice (Figure 1, A–C), whereas trabecular number (WT, 4.3 ± 0.4 per mm; *Nox4*$^{-/-}$, 4.4 ± 0.3 per mm) and separation (WT, 217 ± 23 μm; *Nox4*$^{-/-}$, 207 ± 14 μm) were similar. Compared with their WT littermates, *Nox4*$^{-/-}$ mice also exhibited 30% greater trabecular bone mineral density (BMD) of the distal femur (Figure 1D). Importantly, this effect was specific for *Nox4*, as genetic deletion of *Nox2* or *Nox1* had no effect on BMD (*Nox2*$^{y/+}$, 345.3 ± 12.5 mg/cm^3; *Nox2*$^{y/-}$, 329.0 ± 18.9 mg/cm^3; *Nox1*$^{y/+}$,

Authorship note: Claudia Goettsch and Andrea Babelova contributed equally to this work.

Conflict of interest: The authors have declared that no conflict of interest exists.

Citation for this article: *J Clin Invest.* 2013;123(11):4731–4738. doi:10.1172/JCI67603.

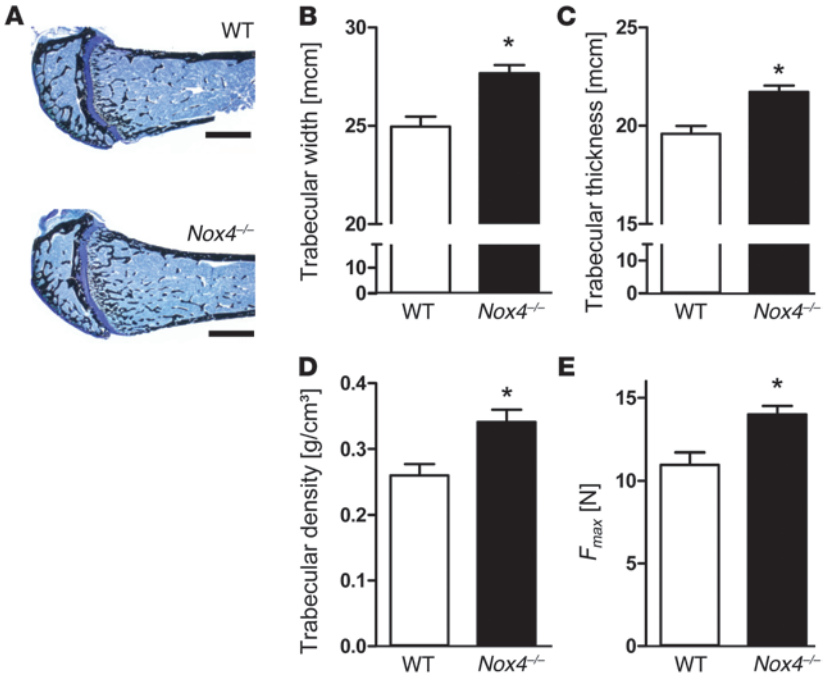

Figure 1
Effect of genetic knockout of *Nox4* on bone density and morphometry. (**A**–**C**) Quantitative histomorphometry of the distal femur of WT and *Nox4*$^{-/-}$ mice (n = 3–5). (**A**) Representative undecalcified section of the distal femur stained with von Kossa. (**B**) Trabecular width. (**C**) Trabecular thickness. (**D**) Trabecular BMD, measured by peripheral quantitative computed tomography (n = 12). (**E**) Biomechanical properties of bone. Bone strength was tested by 3-point bending test (n = 9–11). Scale bars: 1 mm. Data are mean ± SEM. *P < 0.05.

262.2 ± 19.7 mg/cm^3; *Nox1*$^{y/-}$, 268.7 ± 11.0 mg/cm^3; n = 8; P = NS). As a functional consequence, the biomechanical strength of bones from *Nox4*$^{-/-}$ mice was significantly higher than that of WT mice (Figure 1E).

Bone resorption, but not bone formation, depends on NOX4. The elevated BMD in *Nox4*$^{-/-}$ mice suggests that the enzyme either promotes bone resorption or inhibits bone formation. As revealed by calcein labeling, bone formation rate was not altered by genetic deletion of *Nox4* (Figure 2, A and B); additionally, the mineral apposition rate and double-labeled surface were not different between WT and *Nox4*$^{-/-}$ animals (Figure 2C and Supplemental Figure 2A). Moreover, plasma levels of procollagen 1 N-terminal peptide, a marker of osteoblast activity, were similar between WT and *Nox4*$^{-/-}$ mice (Supplemental Figure 2B). As these data exclude a role of NOX4 in osteoblast function, we assumed that NOX4 affects osteoclasts. Indeed, expression of the osteoclast marker osteoclast-associated receptor (OSCAR), but not of the osteoblast marker runt-related transcription factor 2 (RUNX2), was reduced in *Nox4*$^{-/-}$ compared with WT bones (Figure 2D and Supplemental Figure 2C). Accordingly, histochemical analysis of TRAP-positive, multinucleated cells in bone demonstrated a 46% lower osteoclast number in *Nox4*$^{-/-}$ than in WT animals (Figure 2, E and F). In line with this observation, circulating markers of bone resorption, such as TRAP 5b and carboxyterminal collagen cross-links (CTX), were significantly lower in *Nox4*$^{-/-}$ versus WT mice (Figure 2G and Supplemental Figure 2D). Collectively, these data indicate that genetic deletion of *Nox4* leads to reduced formation of osteoclasts and subsequently to reduced bone resorption.

To verify this, the effect of NOX4 on osteoclastogenesis was determined in murine cells in vitro. Bone marrow mononuclear cells (BMNCs) were stimulated with M-CSF and RANKL, and differentiated osteoclasts were identified by their multinucleated morphology and positive TRAP staining. Osteoclast formation was 56% lower in BMNCs of *Nox4*$^{-/-}$ versus WT mice (Figure 2, H and I). This suggests that the lower number of osteoclasts in *Nox4*$^{-/-}$ mice is indeed a consequence of impaired differentiation.

NOX4 is a mediator of RANKL signaling. To provide functional evidence for a role of NOX4 in the process of osteoclast differentiation, NOX4 expression and ROS formation were measured. During RANKL- and M-CSF–stimulated osteoclastogenesis of WT BMNCs, *Nox4* mRNA expression greatly increased (Figure 3A), which was associated with a substantial increase in ROS production. In contrast, ROS formation did not increase in the course of differentiation of cells obtained from *Nox4*$^{-/-}$ mice (Figure 3B), suggesting a potential role of NOX4-derived ROS for RANKL-induced differentiation.

As RANK expression was not different between M-CSF–primed WT and *Nox4*$^{-/-}$ BMNCs (data not shown), we determined the role of NOX4 in RANKL signaling. Treatment of M-CSF–primed murine mononuclear cells with RANKL for 30 hours induced a marked increase in basal cytosolic Ca^{2+} in WT, but not *Nox4*$^{-/-}$, cells. Moreover, catalase prevented the RANKL-induced increase in cytosolic Ca^{2+} in WT cells, but had no effect on basal Ca^{2+} in *Nox4*$^{-/-}$ cells (Figure 3C). Recently, a family of active small-molecule NOX4 inhibitors has been developed (14). Similar to the effects of catalase or *Nox4* deletion, treatment with a compound of this family, GKT137831 (20 μmol/l), prevented the RANKL-induced increase in cytosolic Ca^{2+} in WT cells, without affecting the Ca^{2+} concentration in cells obtained from *Nox4*$^{-/-}$ mice (Figure 3D). These data identified NOX4-derived H_2O_2 as an important mediator of RANKL-induced signaling during osteoclastogenesis.

The transcription factors nuclear factor of activated T cells, cytoplasmic 1 (NFATc1), and activator protein 1 (AP-1) are involved in RANKL-induced osteoclastogenesis (15). NFATc1 activation depends on calcineurin activation, which is directly activated by Ca^{2+} or cleavage by the calcium-dependent protease μ-calpain. Indeed, in response to RANKL, active μ-calpain and nuclear accumulation of NFATc1 increased in M-CSF–primed murine BMNCs, effects that were absent in cells from *Nox4*$^{-/-}$ mice (Figure 3, E and F).

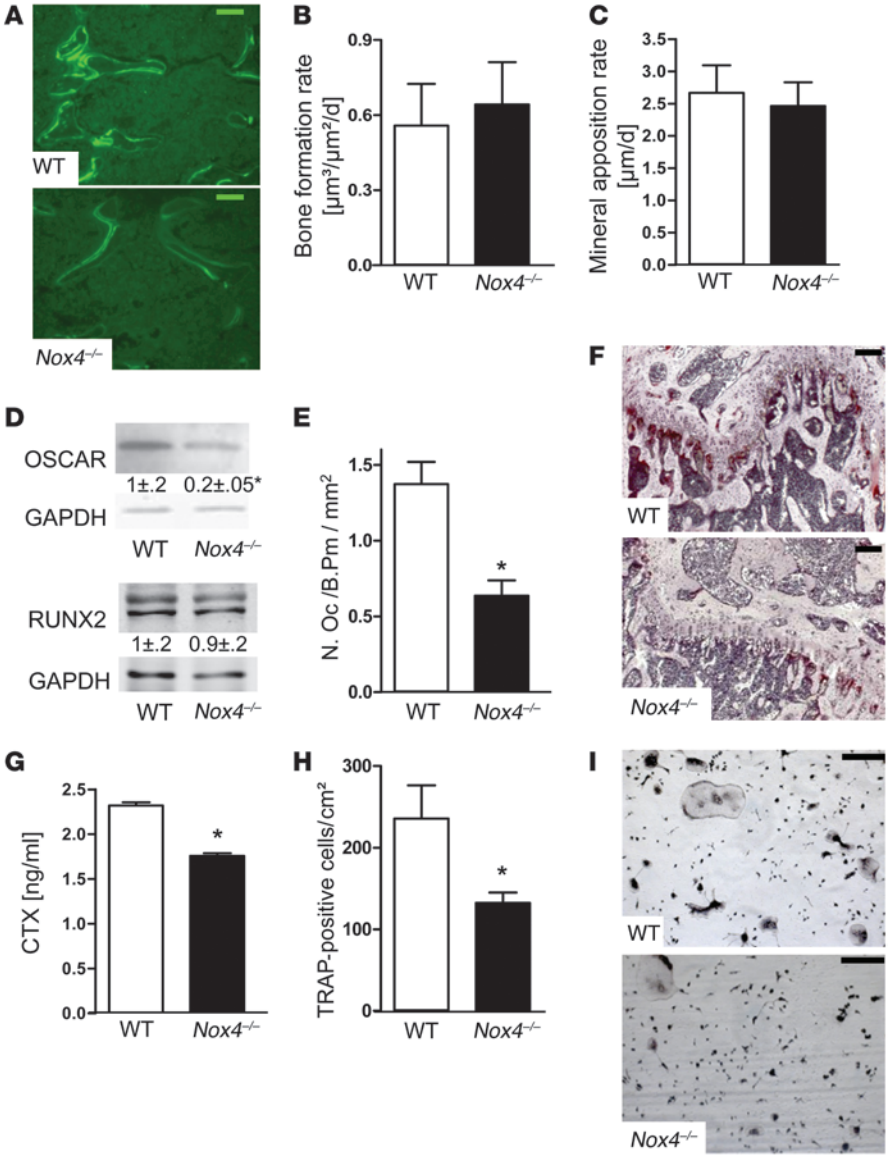

Figure 2
Role of NOX4 in bone remodeling. (**A**) Representative images of calcein-labeled bone surface. (**B**) Bone formation rate and (**C**) mineral apposition rate in bones of WT and *Nox4*$^{-/-}$ mice. (**D**) Western blot analysis and statistical analyses of densitometry (values shown relative to WT control) from femur lysates for OSCAR, RUNX2, and GAPDH as loading control. (**E**) Number of TRAP-positive osteoclasts (N.Oc) per bone perimeter (B.Pm), counted in histomorphometric analysis, and (**F**) representative images of TRAP-stained sections counterstained with Mayer's hemalaun. (**G**) Serum levels of CTX. (**H** and **I**) Number (**H**) and representative images (**I**) of osteoclasts differentiated ex vivo from bone marrow cells of WT and *Nox4*$^{-/-}$ mice, as identified by TRAP staining and multinucleation. Scale bars: 500 μm (**A**); 100 μm (**F** and **I**). Data are mean ± SEM (n = 3–9). *P < 0.05.

Calcineurin expression, in contrast, was not modulated by NOX4 (data not shown). Moreover, AP-1 appeared to be controlled by NOX4: RANKL treatment of M-CSF–primed BMNCs increased JNK phosphorylation in cells from WT, but not *Nox4*$^{-/-}$, cells (WT, 30% ± 1% relative increase after 15-min RANKL stimulation; *Nox4*$^{-/-}$, 1% ± 1% relative increase; n = 3; *P < 0.05). This resulted in a lack of nuclear c-JUN accumulation in *Nox4*$^{-/-}$ cells (Figure 3F). In accordance with these observations, RANKL-mediated *Oscar* induction was attenuated by catalase, by genetic deletion of *Nox4*, and by the calpain inhibitor calpeptin (Figure 3G). Thus, in the course of osteoclastogenesis, NOX4 is required for RANKL-induced activation of the differentiating transcription factors NFATc1 and AP-1.

A SNP of NOX4 is associated with altered bone density and plasma markers for bone turnover in middle-aged women. We next sought to study the contribution of NOX4 to human bone metabolism and performed SNP analyses. For NOX4 rs11018628, a significant association for altered parameters of bone metabolism was found when the dominant TT allele was compared with the combined CC and CT alleles: levels for serum alkaline phosphatase, CTX, and osteocalcin were significantly different between groups in an existing osteoporosis screening study (Tables 1 and 2 and ref. 16). To determine the biological significance of these findings, bone density measurements were performed. Hip BMD T-scores in females, but not males, were significantly higher in the dominant allele; accordingly, there was a trend toward higher areal hip bone density in the female subgroup (Table 3). Although these observations do not prove a direct role of NOX4 in osteoporosis development, they suggest that NOX4 contributes to bone characteristics in humans. As rs11018628 is localized in an intron of NOX4, a direct effect on enzyme activity is not plausible, suggestive of an effect on NOX4 expression. To address this, immortalized EBV-transduced B-lymphocytes of the CC and TT genotypes were obtained from the Coriell Institute (see Methods). *Nox4* mRNA was undetectable in these cells under basal conditions, but increased in the course of differentiation induced by vitamin D3. Importantly, *Nox4* mRNA expression after 3 days

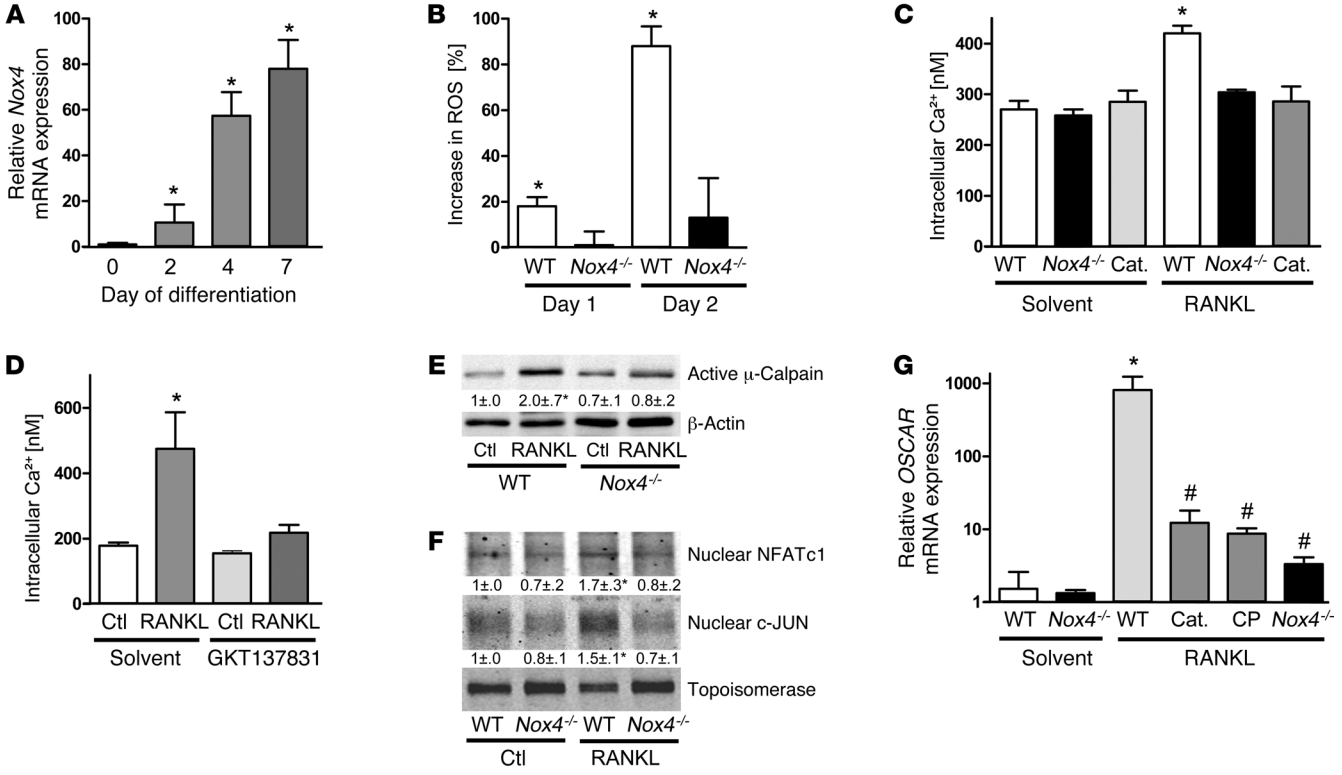

Figure 3
Role of NOX4 in RANKL-induced signaling. (**A**) *Nox4* mRNA expression in murine predifferentiated BMNCs during osteoclastogenesis. (**B**) Relative change in ROS formation, as measured by Amplex Red/HRP, in mononuclear cells harvested from the spleen (splenocytes) stimulated with RANKL for 1 or 2 days. (**C** and **D**) Intracellular Ca^{2+}, measured by Fura-2 fluorescence, in cells pretreated with (RANKL) or without RANKL (solvent) for 30 hours. Cells from WT and *Nox4*$^{-/-}$ mice were treated with and without (**C**) PEG-catalase (Cat.; 50 U/ml) or (**D**) GKT137831 (20 μM). (**E** and **F**) Representative Western blot and statistical analyses of densitometry (values shown relative to WT control) for the indicated proteins from WT and *Nox4*$^{-/-}$ cells with or without (ctl) RANKL prestimulation (50 ng/ml for 30 hours). (**E**) Total cellular lysates. (**F**) Nuclear fraction. (**G**) Relative mRNA expression of *Oscar* in cells treated with and without RANKL, PEG-catalase (50 U/ml), or calpeptin (CP; 20 μM) as indicated. Data are mean ± SEM (n = 5–8). $^{*}P < 0.05$. $^{\#}P < 0.05$ vs. RANKL-treated WT.

of differentiation was significantly higher in cells obtained from subjects carrying the CC versus the TT allele (Supplemental Figure 3). Collectively, these data indicate that NOX4 expression is higher in subjects carrying the CC allele of NOX4 rs11018628, which is associated with increased markers of bone turnover.

Immunoreactivity of NOX4 is increased in human osteoporosis. When human PBMCs were differentiated into osteoclasts in culture, expression of *NOX4* increased during the 21-day protocol, as did that of *NOX1* (Figure 4A and Supplemental Figure 4). Since NOX1 did not affect bone density in vivo (see above), we focused our analyses on NOX4. One major feature of osteoclasts is the resorption of extracellular matrix. In a PIT formation assay, the NOX4 inhibitor GKT137831 dose-dependently prevented the degradation of the matrix (Figure 4, B and C), which suggests that NOX4 is essentially involved in osteoclastogenesis in human cells as well.

To determine the role of NOX4 in human bone metabolism, we compared the expression of the protein in a set of human bones by immunostaining. Staining intensity of NOX4 was markedly higher in bones obtained from patients with untreated osteoporosis compared with healthy bones (mean age, 51 ± 1.5 years; Figure 4, D and E). Moreover, bone samples from patients with Paget disease, a focal disorder of enhanced bone remodeling, also displayed greater NOX4 immunoreactivity.

NOX4 contributes to bone loss in a mouse model of osteoporosis. To test a direct causal link between NOX4 and osteoporosis, we stimulated bone resorption by estrogen withdrawal in mice. Female mice were subjected to ovariectomy, and bone loss was determined 6 weeks later. As expected, the operation induced a reduction of bone density of approximately 25% and an increase in *Oscar* expression in bones, whereas *Runx2* expression remained unchanged (Supplemental Figure 5). After ovariectomy, NOX4 expression gradually increased at the protein and mRNA levels (Figure 5, A and B), again supporting a potential role of NOX4. Therefore, we next studied the effect of acute genetic deletion of *Nox4* by a tamoxifen-activated Cre recombinase (*Nox4*$^{fl/fl}$-*ERT-Cre*$^{+/0}$ mice; see Methods) on bone density. In ovariectomized mice, treatment with tamoxifen itself prevented bone loss to some extent, which was most likely a consequence of the partial agonist activity of tamoxifen on the estrogen receptor, which also shortens osteoclast lifespan and prevents osteocyte apoptosis (17). Despite this, acute *Nox4* deletion in *Nox4*$^{fl/fl}$-*ERT-Cre*$^{+/0}$ animals had an additive inhibitory effect on bone loss (Figure 5C). These data demonstrate that NOX4 is a potential target for the pharmacological prevention of osteoporosis development. In order to verify this aspect, we treated ovariectomized WT mice with the NOX inhibitor GKT137928, administered by

Table 1
General characteristics of the study population for SNP analysis

	Men	Women
Age (yr)	51.08 ± 12.15	61.80 ± 10.70
Weight (kg)	83.3 ± 12.1	66.7 ± 11.3
Height (cm)	176.8 ± 7.0	161.8 ± 6.1
Calcium (mmol/l)	2.48 ± 0.12	2.35 ± 0.11
Phosphate (mg/dl)	2.94 ± 0.58	3.71 ± 0.57
25(OH) vitamin D (ng/ml)	33.22 ± 11.52	32.65 ± 15.07
Alkaline phosphatase (U/l)	69.15 ± 17.50	94.50 ± 35.80
CTX (ng/ml)	0.239 ± 0.134	0.244 ± 0.191
Osteocalcin (ng/ml)	17.7 ± 5.8	7.0 ± 6.7
Parathyroid hormone (pg/ml)	40.7 ± 12.8	28.1 ± 7.7
Lumbar BMD (g/cm^2)	1.016 ± 0.147	0.875 ± 0.173
Lumbar BMD T-score	–0.655 ± 1.329	–1.594 ± 1.436
Lumbar BMD Z-score	–0.150 ± 1.380	–0.075 ± 1.387
Femoral neck BMD (g/cm^2)	0.855 ± 0.121	0.694 ± 0.123
Femoral neck BMD T-score	–0.543 ± 0.893	–1.999 ± 0.122
Femoral neck BMD Z-score	0.292 ± 0.900	–0.265 ± 1.109
Total hip BMD (g/cm^2)	1.017 ± 0.123	0.832 ± 0.145
Total hip BMD T-score	–0.111 ± 0.829	–1.176 ± 1.198
Total hip BMD Z-score	0.304 ± 0.826	0.031 ± 1.085

Data are mean ± SD. n = 228 (men); 180 (women).

daily oral gavage over 6 weeks after ovariectomy, and compared its effect with the gold standard therapeutic bisphosphonate (pamidronate; 10 mg/kg once per week i.p.). Pamidronate massively increased total and trabecular bone density to an extent exceeding even the bone density of the sham-operated mice by approximately 2-fold. The effect of GKT137928, in contrast, was less pronounced, but still attenuated ovariectomy-induced bone loss more than 60% (Figure 5, D and E). Biomechanical strength analysis of the bones was used to determine the functional consequence of this intervention. The breaking strength of bone from mice treated with GKT137928 was significantly higher than that of mice receiving solvent (solvent, 14.1 ± 0.3; GKT137928, 15.1 ± 0.3; n = 8–15; $P < 0.05$). Thus, pharmacological inhibition of NOX4 inhibited bone loss in a model of osteoporosis in mice.

Discussion

Although ROS have been linked to bone loss for many decades (18), our understanding of the mechanisms underlying this phenomenon has changed greatly in recent years. Whereas a concept of redox imbalance and oxidative stress leading to tissue damage was traditionally favored, it is now progressively becoming clear that ROS are pivotal modulators of cell signaling. This concept, however, implies precisely controlled ROS generators, and some of these generators are in fact the NOX proteins (19).

Here we showed that the constitutively active NOX4 is induced during osteoclast differentiation and that its global knockout leads to increased bone density. Alterations in the bones of *Nox4*$^{-/-}$ mice did not affect the compacta, but were restricted to trabecular bone, the site of osteoporosis development. Indeed, acute genetic knockdown of *Nox4* or its pharmacological inhibition attenuated trabecular bone loss in mice after ovariectomy, and in vitro osteoclastogenesis was attenuated after loss of NOX4 activity. These findings are in line with the more general observations that ROS promote osteoclastogenesis in bone marrow–derived cells (12) and in the RAW264.7 macrophage cell line (13).

Given the multiple targets of ROS and the complex alterations in signaling and gene expression occurring in the course of differentiation, it is challenging to define the exact position of NOX4 in the signaling network. RANKL increases intracellular calcium (11) and activates JNK (20) in M-CSF–primed BMNCs, effects that were both attenuated by loss of NOX4 activity in the present study. The increase in intracellular calcium during osteoclast differentiation has been linked to the induction of transient receptor potential cation channel V2 (TRPV2), TRPV5 (21, 22), and sarco(endo)plasmic reticulum Ca^{2+} ATPase (SERCA) (23). Indeed, the activities of these proteins (24, 25) and of other regulators of intracellular calcium are known to be redox sensitive (26, 27). Calcium-induced osteoclast differentiation is mediated by the calcium-stimulated phosphatase calcineurin, which activates nuclear translocation of NFATc1, leading to the expression of OSCAR and other proteins. Activation of calcineurin occurs via a calmodulin-dependent conformational change that releases the autoinhibitory loop of the regulatory subunit calcineurin B (28). An alternative mode of activation is the proteolytic cleavage of the autoinhibitory loop of calcineurin A by μ-calpain, leading to constitutive activation of calcineurin (29). Based on our present findings, we conclude that the RANKL-induced increase in cytosolic Ca^{2+} and μ-calpain activation are NOX4 dependent, and thus calcineurin-mediated nuclear NFATc1 translocation does not occur in *Nox4*-deficient cells. Cooperation of NFATc1 with the transcription factor AP-1 is required for osteoclastogenesis (30). AP-1 requires active JNK MAP kinase, which phosphorylates the AP-1 component c-JUN. MAP kinase activation is among the best-studied of the redox-sensitive processes, which are mediated by transient ROS-mediated oxidation of cysteines in phosphatases (31). However, the sources of ROS — the MAP kinases and phosphatases involved in this process — vary greatly among cell types. NOX4 overexpression in RAW264.7 cells increased JNK phosphorylation (32), and ROS-dependent inhibition of the phosphatase MKP-1 (33), which dephosphorylates JNK in osteoclasts (34), has been implicated in this process in fibroblasts.

Although eventually, only studies in humans treated with NOX4 inhibitors will unravel the importance of this NOX for bone loss, several lines of evidence in the present study suggest NOX4 as a possible pharmacological target for the treatment of osteoporosis: (a) acute genetic deletion or pharmacological inhibition of NOX4 attenuated bone loss in the murine ovariectomy model, (b) NOX4 immunoreactivity was increased in osteoporotic bones, and (c) SNP analysis suggested that NOX4 expression in humans is associated with altered parameters of bone metabolism. Thus, the present study provided evidence on multiple levels to qualify NOX4 as a novel pharmacological target for the treatment of bone loss. With GKT137831 and GKT137928, the first specific NOX inhibitors without antioxidant properties

Table 2
Effect of the SNP rs11018628 on markers of bone metabolism

	CC+CT	TT	*P*
Alkaline phosphatase (U/l)	86.8 ± 28.1	78.7 ± 29.7	0.018
CTX (ng/ml)	0.285 ± 0.125	0.234 ± 0.190	0.002
Osteocalcin (ng/ml)	10.07 ± 6.79	9.33 ± 11.07	0.013

Data are mean ± SD. n = 1 (CC); 56 (CT); 351 (TT).

Table 3
Effect of the SNP rs11018628 in the female subgroup

	CC+CT	TT	*P*
Bone density parameters[A]			
Hip T-score	–1.574 ± 1.550	–1.095 ± 1.102	0.048
Hip Z-score	–0.258 ± 1.384	0.089 ± 1.009	0.091
Hip density (g/cm^2)	0.786 ± 0.186	0.841 ± 0.134	0.057
Bone metabolism markers			
CTX (ng/ml)[B]	0.261 ± 0.097	0.241 ± 0.204	0.033
Osteocalcin (ng/ml)[C]	7.17 ± 1.90	6.93 ± 7.33	0.002

Data are mean ± SD. [A]*n* = 29 (CC+CT); 143 (TT). [B]*n* = 27 (CC+CT); 141 (TT). [C]*n* = 29 (CC+CT); 147 (TT).

and good biocompatibility have become available (35) and are currently in preclinical testing. Although the isoform specificity of the compounds is limited, our experiments performed in *Nox1*- and *Nox2*-deficient mice as well as previous work (13) excluded NOX1 and NOX2 as mediators of osteoclast function under physiological conditions. Nevertheless, under different circumstances, such as inactivation, atrophy, or inflammation, other sources of ROS, like NOX2 or mitochondria, might be relevant for bone loss (36).

In conclusion, we provide a direct link between NOX4 and bone loss: NOX4 expression was increased in osteoporotic bone in humans, and SNP analyses linked NOX4 to bone metabolism. In mice, in vivo inhibition or knockdown of NOX4 prevented bone loss secondary to estrogen withdrawal, and global *Nox4*-knockout mice exhibited increased bone density. These results suggest that bone loss disorders could be attenuated by inhibition of NOX4.

Methods

For details of BMD measurement, bone histology and histomorphometry, bone biomechanics analysis, cell culture and ex vivo cell differentiation, pit formation, amplex red assay for H_2O_2 production, intracellular calcium measurement, immunoblotting, quantitative PCR, surgical procedures, and statistical analyses, see Supplemental Methods.

Studies using human cohorts and cells. The cohorts at Graz University were studied (16, 37), and genotyping for NOX4 SNPs was carried out by TaqMan fluorogenic 5′ exonuclease assay. Immortalized B lymphocytes carrying the alleles TT or CC were obtained from the Coriell Institute. The following cell lines were obtained from the NIGMS Human Genetic Cell Repository at the Coriell Institute for Medical Research: GM12864, GM12874, GM18571, GM18573, GM18576, GM18577, GM18972, GM18976, GM18978, GM18969, GM19138, GM19145, GM19222, GM19223, GM19210, and GM19238.

Mice and animal procedures. Mice were bred in our animal facility. The *Nox2*$^{y/-}$ and *Nox1*$^{y/-}$ founders of our colonies were obtained from Charles River and provided by K.H. Krause (University of Geneva, Geneva, Switzerland), respectively. *Nox4*$^{-/-}$ mice were generated by targeted deletion of the translation initiation site and of exons 1 and 2 of *Nox4* (Genoway) (38). Tamoxifen-inducible *Nox4*-knockout mice (*Nox4*$^{fl/fl}$-*Cre-ERT2*$^{+/0}$) were produced by crossing homozygous *Nox4*$^{fl/fl}$ mice with tamoxifen-inducible *Cre-ERT2*$^{+/0}$ mice (39). In all experiments, littermate WT and knockout animals were used.

Osteoporosis was induced by ovariectomy, and bone composition was studied 6 weeks after surgery (40). Pharmacological inhibition of NOX4 was

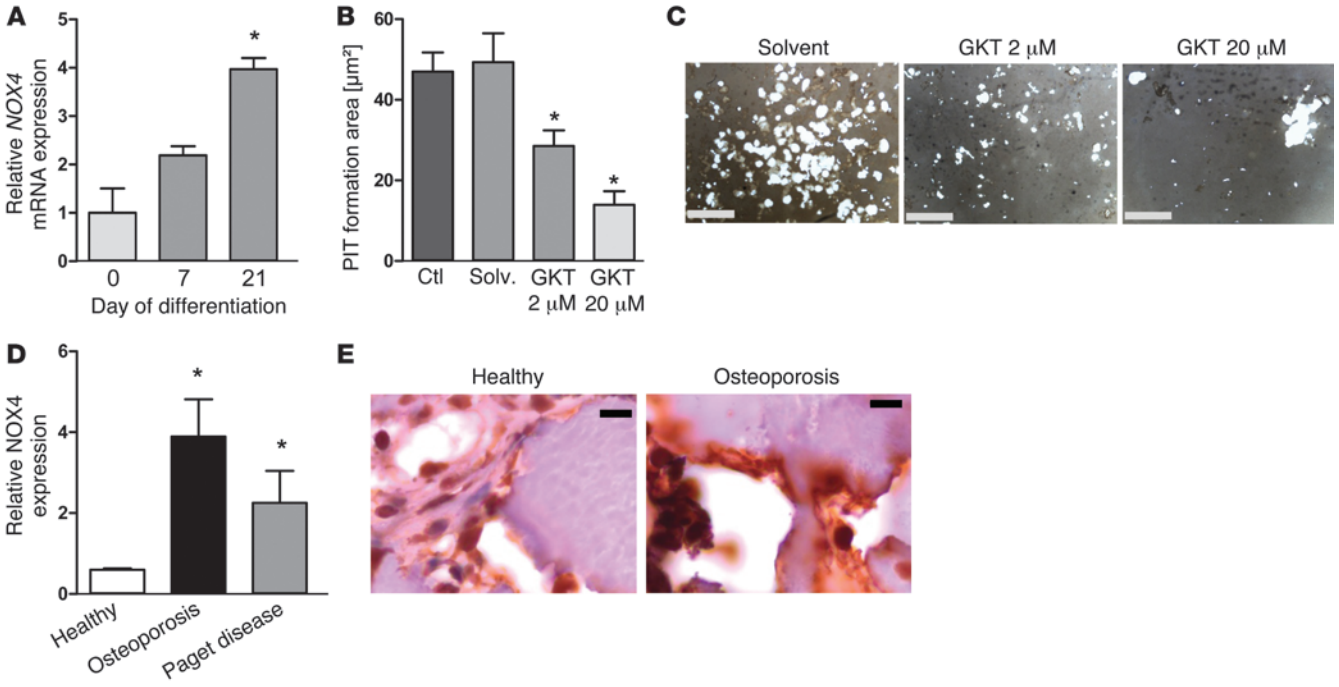

Figure 4
Role of NOX4 in human bone loss. (**A**) *Nox4* mRNA expression in the course of differentiation of human precursor cells into osteoclasts. (**B**) Statistical analysis and (**C**) representative images of PIT formation assays of human PBMCs treated with RANKL with or without GKT137831. (**D**) Intensity of NOX4 staining in human bone material from healthy subjects and patients with osteoporosis or Paget disease. (**E**) Representative images of bone slides from a healthy subject and an osteoporotic patient stained for NOX4 (brown) and counterstained with hemalaun (violet). Scale bars: 1 mm (**C**); 50 μm (**E**). Data are mean ± SEM (*n* = 3–6). *$P < 0.05$.

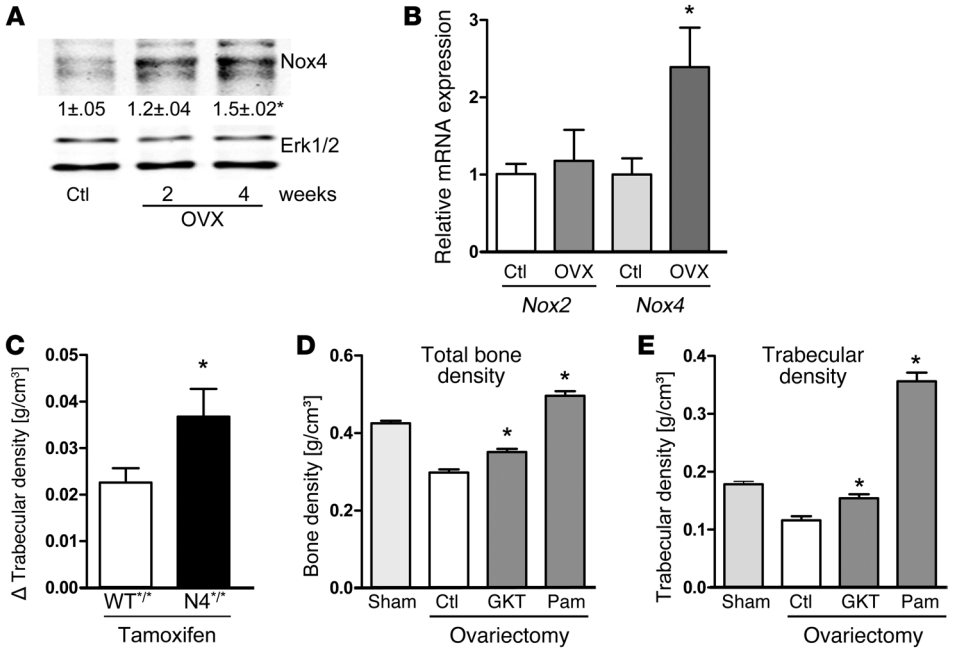

Figure 5

Role of NOX4 for bone loss in the murine model of osteoporosis. (**A**) Western blot analyses and statistical analyses of densitometry (values shown relative to healthy control) of NOX4 protein expression in bones of healthy and ovariectomized mice. (**B**) mRNA expression of *Nox2* and *Nox4* ($n = 3–5$). *$P < 0.05$. (**C**–**E**) Bone density of the distal femur 6 weeks after ovariectomy. (**C**) Trabecular density increase in tamoxifen-treated WT (WT*/*) and *Nox4*$^{fl/fl}$-*ERT2-Cre*$^{+/0}$ (N4*/*) mice relative to ovariectomized, untreated WT animals ($n = 8–12$). *$P < 0.05$. (**D**) Total and (**E**) trabecular bone density, measured within 2 mm of the tibia plateau, in WT animals treated with solvent (Ctl), GKT137928 (GKT; 20 mg/kg/d), or pamidronate (Pam; 10 mg/kg once a week i.p.) beginning 2 days after ovariectomy ($n = 8–15$). Data are mean ± SEM. *$P < 0.05$ vs. solvent control.

achieved by administration of the compound GKT137928 (20 mg/kg/d; provided by Genkyotex) by daily gavage. Genetic deletion of *Nox4* in *Nox4*$^{fl/fl}$-*Cre-ERT2*$^{+/0}$ mice was induced by injection of tamoxifen (40 mg/kg i.p. on 3 consecutive days). Interventions were started 2 days after ovariectomy.

Statistics. All values are expressed as mean ± SEM, with the exception of SNP data, which are expressed as mean ± SD. Normal distribution of data was analyzed by Kolmogorov-Smirnov test. Categorical variables were compared by χ^2 test, numeric values were compared by 2-tailed Student's *t* test, and multiple-group comparisons were made by ANOVA. Data showing unequal variance or lacking normal distribution were analyzed by Wilcoxon rank-sum test or Kruskal Wallis test. A *P* value less than 0.05 was considered statistically significant.

Study approval. Animal experiments in Frankfurt, Germany, were approved by local governmental authorities (approval no. F28/20) and performed in accordance with animal protection guidelines. Human bone samples were obtained following approval by the Institutional Review Board of the Dresden Medical Faculty (EK245082010). Protocol procedures for cross-sectional study for SNP analyses were approved by the local Ethics Committee of the Medical University of Graz. Written informed consent was obtained from all study participants.

Acknowledgments

We thank Ramona Famulla, Jasmin Kohout, Isabella Schlöffel, Nicole Pacyna, Cindy Höper, and Sina Bätz for excellent technical support; Gabriele Lehmann, Voahanginirina Randriamboavonjy, Johann Isaack, Caroline Seebach, and Dirk Henrich for helpful discussion; and Genkyotex SA for providing GKT137831 and GKT137928. This work was supported by the MeDDrive33 program of the Medical Faculty of the Technical University of Dresden (to C. Goettsch); by Deutsche Forschungsgemeinschaft grants SFB815/TP1 (to K. Schröder), SFB 834/TP2 (to R.P. Brandes), GO1801/4-1 (to C. Goettsch and L.C. Hofbauer), and FOR1586 HO 1875/12-1 and FOR1586 HO 1875/13-1 (to L.C. Hofbauer); by the Hugelschaffner-Stiftung (to K. Schröder); by DFG excellence cluster ECCPS (to R.P. Brandes and N. Weissmann); and by Goethe University (to K. Schröder). This work was partly supported by BioPersMed (COMET K-project 825329), which is funded by the Austrian Federal Ministry of Transport, Innovation and Technology (BMVIT) and the Austrian Federal Ministry of Economics and Labour/Federal Ministry of Economy, Family and Youth (BMWA/BMWFJ); by the Styrian Business Promotion Agency (SFG); and by Genkyotex Innovation SAS.

Received for publication October 30, 2012, and accepted in revised form August 15, 2013.

Address correspondence to: Katrin Schröder, Institut für Physiologie I, Haus 75, 2.OG Fachbereich Medizin, Goethe-Universität, Theodor-Stern-Kai 7, 60590 Frankfurt am Main, Germany. Phone: 49.69.6301.83660; Fax: 49.69.6301.7668; E-mail: schroeder@vrc.uni-frankfurt.de.

1. Hsu H, et al. Tumor necrosis factor receptor family member RANK mediates osteoclast differentiation and activation induced by osteoprotegerin ligand. *Proc Natl Acad Sci U S A*. 1999;96(7):3540–3545.
2. Woo KM, Kim HM, Ko JS. Macrophage colony-stimulating factor promotes the survival of osteoclast precursors by up-regulating Bcl-X(L). *Exp Mol Med*. 2002;34(5):340–346.
3. Kong YY, et al. OPGL is a key regulator of osteoclastogenesis, lymphocyte development and lymph-node organogenesis. *Nature*. 1999;397(6717):315–323.
4. Lacey DL, et al. Osteoprotegerin ligand modulates

murine osteoclast survival in vitro and in vivo. *Am J Pathol*. 2000;157(2):435–448.
5. Burgess TL, et al. The ligand for osteoprotegerin (OPGL) directly activates mature osteoclasts. *J Cell Biol*. 1999;145(3):527–538.
6. Yan T, Riggs BL, Boyle WJ, Khosla S. Regulation of osteoclastogenesis and RANK expression by TGF-β1. *J Cell Biochem*. 2001;83(2):320–325.
7. Sturrock A, et al. Transforming growth factor-beta1 induces Nox4 NAD(P)H oxidase and reactive oxygen species-dependent proliferation in human pulmonary artery smooth muscle cells. *Am J Physiol Lung Cell Mol Physiol*. 2006;290(4):L661–L673.
8. Takac I, et al. The E-loop is involved in hydrogen peroxide formation by the NADPH oxidase Nox4. *J Biol Chem*. 2011;286(15):13304–13313.
9. Schroder K, Wandzioch K, Helmcke I, Brandes RP. Nox4 acts as a switch between differentiation and proliferation in preadipocytes. *Arterioscler Thromb Vasc Biol*. 2009;29(2):239–245.
10. Garrett IR, Boyce BF, Oreffo RO, Bonewald L, Poser J, Mundy GR. Oxygen-derived free radicals stimulate osteoclastic bone resorption in rodent bone in vitro and in vivo. *J Clin Invest*. 1990;85(3):632–639.
11. Hwang SY, Putney JW. Calcium signaling in osteoclasts. *Biochim Biophys Acta*. 2011;1813(5):979–983.
12. Lee NK, et al. A crucial role for reactive oxygen species in RANKL-induced osteoclast differentiation. *Blood*. 2005;106(3):852–859.
13. Sasaki H, et al. NADPH oxidase-derived reactive oxygen species are essential for differentiation of a mouse macrophage cell line (RAW264.7) into osteoclasts. *J Med Invest*. 2009;56(1–2):33–41.
14. Laleu B, et al. First in class, potent, and orally bioavailable NADPH oxidase isoform 4 (Nox4) inhibitors for the treatment of idiopathic pulmonary fibrosis. *J Med Chem*. 2010;53(21):7715–7730.
15. Asagiri M, Takayanagi H. The molecular understanding of osteoclast differentiation. *Bone*. 2007; 40(2):251–264.
16. Obermayer-Pietsch BM, et al. Genetic predisposition for adult lactose intolerance and relation to diet, bone density, and bone fractures. *J Bone Miner Res*. 2004;19(1):42–47.
17. Manolagas SC. Steroids and osteoporosis: the quest for mechanisms. *J Clin Invest*. 2013;123(5):1919–1921.
18. Banfi G, Iorio EL, Corsi MM. Oxidative stress, free radicals and bone remodeling. *Clin Chem Lab Med*. 2008;46(11)1550–1555.
19. Jiang F, Zhang Y, Dusting GJ. NADPH oxidase-mediated redox signaling: roles in cellular stress response, stress tolerance, and tissue repair. *Pharmacol Rev*. 2011;63(1):218–242.
20. Zhou S, et al. BAPTA-AM, an intracellular calcium chelator, inhibits RANKL-induced bone marrow macrophages differentiation through MEK/ERK, p38 MAPK and Akt, but not JNK pathways. *Cytokine*. 2010;52(3):210–214.
21. Kajiya H, et al. RANKL-induced TRPV2 expression regulates osteoclastogenesis via calcium oscillations. *Cell Calcium*. 2010;48(5):260–269.
22. Chamoux E, Bisson M, Payet MD, Roux S. TRPV-5 mediates a receptor activator of NF-kappaB (RANK) ligand-induced increase in cytosolic Ca2+ in human osteoclasts and down-regulates bone resorption. *J Biol Chem*. 2010;285(33):25354–25362.
23. Mentaverri R, Kamel S, Brazier M. Involvement of capacitive calcium entry and calcium store refilling in osteoclastic survival and bone resorption process. *Cell Calcium*. 2003;34(2):169–175.
24. Miller BA, Zhang W. TRP channels as mediators of oxidative stress. *Adv Exp Med Biol*. 2011;704:531–544.
25. Tong X, Hou X, Jourd'heuil D, Weisbrod RM, Cohen RA. Upregulation of Nox4 by TGF{beta}1 oxidizes SERCA and inhibits NO in arterial smooth muscle of the prediabetic Zucker rat. *Circ Res*. 2010; 107(8):975–983.
26. Gooch JL, Gorin Y, Zhang BX, Abboud HE. Involvement of calcineurin in transforming growth factor-beta-mediated regulation of extracellular matrix accumulation. *J Biol Chem*. 2004;279(15):15561–15570.
27. Kim MS, et al. RANKL-mediated reactive oxygen species pathway that induces long lasting Ca2+ oscillations essential for osteoclastogenesis. *J Biol Chem*. 2010;285(10):6913–6921.
28. Klee CB, Ren H, Wang X. Regulation of the calmodulin-stimulated protein phosphatase, calcineurin. *J Biol Chem*. 1998;273(22):13367–13370.
29. Pare G, et al. Novel associations of CPS1, MUT, NOX4, and DPEP1 with plasma homocysteine in a healthy population: a genome-wide evaluation of 13 974 participants in the Women's Genome Health Study. *Circ Cardiovasc Genet*. 2009;2:142–150.
30. Asagiri M, et al. Autoamplification of NFATc1 expression determines its essential role in bone homeostasis. *J Exp Med*. 2005;202(9):1261–1269.
31. Cross JV, Templeton DJ. Regulation of signal transduction through protein cysteine oxidation. *Antioxid Redox Signal*. 2006;8(9–10):1819–1827.
32. Yang S, Zhang Y, Ries W, Key L. Expression of Nox4 in osteoclasts. *J Cell Biochem*. 2004;92(2):238–248.
33. Liu RM, et al. Oxidative modification of nuclear mitogen-activated protein kinase phosphatase 1 is involved in transforming growth factor beta1-induced expression of plasminogen activator inhibitor 1 in fibroblasts. *J Biol Chem*. 2010;285(21):16239–16247.
34. Carlson J, et al. Role of MKP-1 in osteoclasts and bone homeostasis. *Am J Pathol*. 2009;175(4):1564–1573.
35. Aoyama T, et al. Nicotinamide adenine dinucleotide phosphate oxidase in experimental liver fibrosis: GKT137831 as a novel potential therapeutic agent. *Hepatology*. 2012;56(6):2316–2327.
36. Loeser RF. Aging and osteoarthritis. *Curr Opin Rheumatol*. 2011;23(5):492–496.
37. Gugatschka M, et al. Molecularly-defined lactose malabsorption, milk consumption and anthropometric differences in adult males. *QJM*. 2005;98(12):857–863.
38. Zhang M, et al. NADPH oxidase-4 mediates protection against chronic load-induced stress in mouse hearts by enhancing angiogenesis. *Proc Natl Acad Sci U S A*. 2010;107(42):18121–18126.
39. Indra AK, et al. Temporally-controlled site-specific mutagenesis in the basal layer of the epidermis: comparison of the recombinase activity of the tamoxifen-inducible Cre-ER(T) and Cre-ER(T2) recombinases. *Nucleic Acids Res*. 1999;27(22):4324–4327.
40. Chang J, et al. Inhibition of osteoblastic bone formation by nuclear factor-kappaB. *Nat Med*. 2009; 15(6):682–689.